Proliferative arrest induces neuronal differentiation and innate immune responses in normal and Creutzfeldt-Jakob Disease agent (CJ) infected rat septal neurons

Nathan Pagano, Gerard Aguilar Perez[1], Rolando Garcia-Milian[2] and Laura Manuelidis*

Yale University Medical School
333 Cedar Street, Room FMB11
New Haven CT 06510
203-785-4442

Short Title: Proliferative arrest, neuronal differentiation and innate immunity in normal and CJ infected septal neurons

Key words: post-mitotic neurons, reversible arrest; neural fate; latent infection; innate immunity; interferons; cytokines/chemokines; amyloid anti-viral defenses; proliferative escape; cell transformation; epigenetic imprinting; Alzheimer's disease;

* To whom correspondence should be addressed: laura.manuelidis@yale.edu

[1] Current address Laboratory of Molecular Neuroscience, German Center for Neurodegenerative Diseases (DZNE), 10117 Berlin, Germany.
[2] Bioinformatics Support Hub, Yale Medical Library, Yale School of Medicine

ABSTRACT

Rat post-mitotic septal neurons, engineered to proliferate and arrest under physiological conditions can be maintained for weeks without cytotoxic effects. Nine independent cDNA libraries were made to follow arrest-induced neural differentiation and innate immune responses in normal uninfected and CJ agent infected septal neurons for weeks. CJ infection created a non-productive latent (CJ-) and a productive (CJ+) high infectivity model (10 logs/gm). Arrest of normal uninfected cells upregulated a plethora of anti-proliferative transcripts and known neuronal differentiation transcripts (e.g., Agtr2, Neuregulin-1, GDF6, SFRP4 and Prnp). Notably, many activated IFN innate immune genes were simultaneously upregulated (e.g., OAS1, RTP4, ISG20, GTB4, CD80, cytokines, chemokines and complement) along with clusterin (CLU) that binds misfolded proteins. Arrest of latently infected CJ- cells induced even more profound global transcript differences. CJ+ cells markedly downregulated the anti-proliferative controls seen in arrested normal cells. CJ+ infection also suppressed neuronal differentiation transcripts, including Prnp which is essential for CJ agent infection. Additionally, IFN and cytokine/chemokine pathways were also strongly enhanced. Analysis of the 342 CJ+ unique transcripts revealed additional innate immune and anti-viral-linked transcripts, e.g., Il17, ISG15, and RSAD2 (viperin). These data show: 1) innate immune transcripts are produced by normal neurons during differentiation; 2) CJ infection enhances and expands anti-viral responses; 3) non-productive latent infection can epigenetically imprint many proliferative pathways to thwart complete arrest. Consequently, human blood and intestinal myeloid peripheral cells that are latently infected (silent) for many years may be stimulated in vitro to produce CJ+ linked diagnostic transcripts.

INTRODUCTION

There are relatively few papers analyzing cDNA libraries of normal differentiating neurons in culture as they transition from a proliferative to an arrested G1 state. Post-mitotic neuron differentiation in animals takes place over many days with differentiation times determined by species and neuronal cell type (1). Studies of neuron differentiation in brain are complicated by cellular and humoral complexity. Neuroectodermal cells (as astrocytes), along with vascular endothelium, microglia, and blood borne factors (serum molecules and hormones) can have multiple effects on core neuronal differentiation and cell fate programs. Cultured rat post-mitotic septal (SEP) neurons immortalized with a temperature sensitive (ts) SV40 construct provide a powerful model for studies of neural differentiation over a 3-4 week period without these complications (2, 3). We are not aware of any reports of post-mitotic neurons where differentiation can be reversibly turned on and off for weeks, a feature that can be particularly informative for understanding latent viral infections.

SEP cells proliferate at 33°C and can be physiologically arrested at 37.5 ^{o}C in 2 % serum. Arrested cells stop synthesizing DNA by 4-6 days post-arrest, as assessed by BrdU incorporation in nuclei, and these cells can be maintained in an arrested state by refeeding every 2 days for >75 days without reverting to a proliferative state (4). During this time, cell-to-cell contacts and neural markers increase along with host prion protein (PrP) assayed on western blots, and host gene transcripts (Prnp) assayed by RT/qPCR (4, 5). PrP is a neural differentiation marker that increases during synaptogenesis and localizes to membranes by electron microscopy (6). It is also a required host factor for infection in CJD and other Transmissible Spongiform Encephalopathies (TSEs) (7) and its misfolded or amyloid form is a marker of disease. RT/qPCR studies of normal SEP cells were limited previously to a few chosen molecular markers and were insufficient to address more global changes, some of which may be unsuspected. Large scale cDNA libraries were made here to reveal transcripts and networked pathways induced during established arrest. Because previous RT/qPCR studies of normal SEP neurons showed arrest induced upregulation of β-interferon (β-IFN), a classical innate immune response (4), cDNA libraries were interrogated to confirm and expand additional immune changes that might accrue in these normal SEP cell samples during neuronal differentiation.

Parallel studies of normal rat SEP cells infected and those infected by rat passaged human FU-CJD agent (CJ) (5, 8) provided an intriguing comparison: arrested CJ infected SEP cells produced persistent high

titers of the infectious agent (9.7 logs/gm for 120 days) as well as pathologic PrP amyloid without visible cytotoxic or neurodegenerative stigmata observed in high infectivity CJD brain. Misfolded PrP amyloid appears late in disease brain, after the CJ agent has silently replicated to high levels, e.g. 8.5 logs/gm (9). When highly infectious (CJ+) SEP cells are allowed to proliferate at 33°C they rapidly lose 5 logs of infectivity, i.e. <1 infectious dose/gm (5). To determine if these proliferating SEP cells with no detectable infectivity (CJ-) were latently infected, they were re-arrested. Again they produced very high levels of infectious agent (10 logs/gm), proving that latent, silent non-productive infection remained in the CJ- proliferating cells. Re-arrested CJ+ cells rapidly displayed detectable PrP amyloid along with 60-fold elevated β–IFN transcripts (4) whereas arrested Nl controls never spontaneously developed PrP amyloid. Multiple RNA samples from these proliferating CJ- and re-arrested CJ+ cells were used to make libraries for bioinformatic analysis of additional transcripts and pathways that are altered during non-productive latent and productive CJ infection. Latent infections can be very extended in infected people. For example, cannibalism associated kuru in New Guinea can take >10 years to produce neurological disease after peripheral exposure (10), and sporadic CJD (sCJD) contaminated growth hormone infections can remain latent for at least 30 years (4), with recorded latencies of 38 years (11). This is relevant because sCJD infections, unlike kuru, have not disappeared. Since not all people exposed to sCJD growth hormone develop disease, a remaining subset of the population exposed to sCJD may continue to harbor silent infections that have not been detected. Latent states of infection in TSEs (non-proliferative to silent productive a states) have largely been forgotten in studies focusing on PrP amyloid.

Latency in CJD and other TSEs is informed by experimental animal studies. Endemic sheep scrapie, a neurodegenerative disease recognized for over 500 years, human sporadic Creutzfeldt-Jakob Disease (sCJD), and epidemic “mad cow” disease (BSE) belong to the group of Transmissible spongiform encephalopathies (TSEs) (12). Fundamental infectious and pathologic features of TSEs were first demonstrated in 1936 by serial passage of sheep scrapie brain (12). In these experiments the infectious agent was referred to as a virus or a slow virus because of its undeniably virus-like biology (see below). Because the molecular nature and strain-defining attributes of the infectious particle remain unresolved, we use the term infectious agent. Notably, misfolded non-infectious PrP amyloid can’t be distinguished from infectious PrP amyloid e.g., (13), and TSE

infectious particles, as viruses, require nucleic acids (14). The word virus below is used according to the authors' designation.

Wilson showed the scrapie virus (in clarified brain homogenates) efficiently passed through 0.41μ filters, and caused disease via various inoculation routes, e.g., intracerebral, intravenous, cutaneous (15). Successful transmission of the sheep scrapie virus to rodents in the 1960s, critical for pathogenesis studies, showed the incubation time to disease after inoculation (latency) was dependent on dose, route and species susceptibility, and lymphoid tissue infections (a latent reservoir) preceded brain infections by 10 weeks (16). Transmission of sCJD to small animals in the 1970s added other medically relevant findings such as infection by white blood cells and lack of maternal transmission (17). As in scrapie, different CJD agent strains were identified by latency and the distribution and severity of brain lesions (12, 18). In normal mice the sCJD agent is slow and produces minimal lesions restricted to the medial thalamus while the Asiatic FU-CJD strain replicates rapidly and produces widespread destructive lesions. Despite this difference in virulence, a 4 log difference in infectivity but only a 1 log difference in PrP amyloid, both human CJD agents show indistinguishable PrP amyloid characteristics. Typically PrP amyloid is not strain-specific (19) but cell-type specific (20). Powerful virulence for a specific species and/or PrP pathogenetic features of sCJD and FU-CJD were further demonstrated. Using a classical viral vaccination strategy inoculated low infectivity slow sCJD agent prevented superinfection by the high infectivity fast FU-CJD agent in mice, and this was reproducible in cell cultures where various scrapie agents were also compared (19, 21, 22). These strain findings are of relevance because in principle, latent infection could underlie resistance to infection by more virulent infectious and/or neuropathogenic agent features of high PrP amyloid without infectivity (13).

Since the differentiation of various types of neurons is exquisitely connected to specific sequential times of development, we compared representative early and later post-arrest days in parallel studies of uninfected and CJD infected SEP cells. To ensure the high reproducibility of major transcript and pathway changes, different independent SEP cell passage groups at multiple days after arrest were compared using the most relevant and representative time points based on previous RT/qPCR, protein and shared cellular marker studies (3, 4).

MATERIAL AND METHODS

Cell Culture characterizations: All experiments and cultures used to make cDNA libraries were previously described in detail [4]. Briefly, low passage post-mitotic rat Septal (SEP) neurons, immortalized with a temperature sensitive ts-SV40 T antigen (subclone e422, [1]), were passaged every 4 days at 1:4 in a proliferating state at 33°C in 10% serum-DMEM. To induce and maintain arrest, cells were cultured in 2% serum-DMEM at 37.5^{o}C and refed every 2 days without splitting. Normal arrested cells became 95% stationary by day 2, shown by cessation of BrdU incorporation into DNA and loss of SV40 T antigen protein (Tag) e.g., [2]. With arrest, prion protein (PrP) progressively increases to 15-20x the normal uninfected level in SEP cells from passages 7, 17 and 25 [4], and these arrested and parallel controls were used here for cDNA libraries and analyses. Briefly, thawed untreated normal cells from these different passages were either allowed to proliferate, or maintained in an arrested state for the indicated days of each passage set. Independent groups of parallel proliferating and arrested cells from the same day were compared. Proliferating and arrested cells from these 3 independent passages showed comparable patterns of PrP, SV40 Tag and β-IFN changes. In Fig. 1A (see Results) summarizes these proliferating control uninfected cells in light green (Prol/Nl) with their parallel arrested cells sampled on the same day in darker green (Arst/Nl).

Fig. 1A also shows two CJD groups with control proliferating cells (Prol/CJ-) in light orange, and their parallel re-arrested counterparts in dark orange (Arst/CJ+). More specifically, proliferating SEP cells that had been infected with FU-CJD rat brain homogenate (8) that were arrested for 75 days attained a high titer of 5 tissue culture infectious doses per cell (TCID), equivalent to 5E9 infectious particles/gm where 1gm of brain contains 10^9 cells in standardized assays as described (5, 23, 24). These high infectivity cells were frozen at passage 17 (p17). They were then thawed and allowed to proliferate for 3 additional passages. Even with 1 passage of release from arresting conditions, the high CJD infectivity of 5 TCID/cell was substantially lost and reduced to 2 TCID/1,000 cells, i.e., a loss of 3 logs (5). Thus, proliferating SEP cells are designated Prol/CJ- to indicate they lost all detectable infectivity after further passaging these samples (4). These CJ- controls were pertinent because the effects of previous high FU-CJD infection might alter standard normal SEP cell characteristics. In the current experiments, at passage 3 after thawing, proliferating FU-CJD SEP cells were re-arrested and maintained in parallel with their CJ- controls. By 6 days and 34 days post-arrest their infectivity

increased to 2 and >10 TCID per cell respectively (>10 logs/gm) in standard GT1 indicator cell assays as depicted [4]. TCID infectivity assays correlate well with LD_{50} animal agent titrations, and re-inoculation of infected cells also reproduce their strain-specific characteristics in mice. These high infectivity FU-CJD SEP cells are designated Arst/CJ+. Selection of passage and sample days for both normal and CJD groups here were based on protein and RT/qPCR cDNA analyses as graphically detailed [4] for elevated β-interferon, Prnp and absent Tag RNAs in addition to relevant protein changes including protease resistant PrP amyloid.

RNA sequencing: Brett Robb and staff at New England Biolabs generously constructed the cDNA libraries and performed the RNA sequencing for the above samples. Between 72-92 ng of RNA per sample was subjected to rRNA depletion via the NEBNext® rRNA Depletion Kit v2 (Human/Mouse/Rat; NEB #E7400) using the manufacturer's protocol except that a Monarch® RNA Cleanup Kit (10 µg; NEB# T2030) was used to purify the rRNA-depleted RNA instead of magnetic beads. The rRNA-depleted RNA was converted [15] into Illumina-compatible DNA libraries via the NEBNext® Ultra™ II Directional RNA Library Prep with Sample Purification Beads kit (NEB# E7765) using the manufacturer's protocol for use with rRNA-depleted RNA and NEBNext® Multiplex Oligos for Illumina® (NEB# E6448). Samples were pooled and sequenced 2x150 nt paired-end on an Illumina® Novaseq 6000 instrument.

RNA bioinformatic analysis: Partek™ Flow™ software (version 11) bulk RNA-seq pipeline was used for data analysis. In summary, trimmed reads were aligned to the Rnor_6.0 (rn6) genome reference using STAR (25) (version 2.7.8), and subsequently Partek E/M algorithm (26) was used to count reads mapping to the genes from Ensembl release 95. We applied the DESeq2 normalization method and top 1000 genes by variance were analyzed for PCA. Heatmaps show row-normalized relative gene expression z-scores across columns. Qlucore Omics Explorer (Qlucore, Lund, Sweden), a dynamic, interactive visualization-guided bioinformatics program with a built-in statistical platform was used for data visualization. Differential expression was performed using the DESeq2 (27) method. The cutoff value to select differentially expressed genes was Log2ratio ≥ |0.5|, FDR $p<0.05$ (28). A copy of the dataset was stored in the National Center for Biotechnology Information, Gene Expression Omnibus database: GSE272571

Functional analysis: Overrepresented pathways, biological functions, upstream regulators, and biological networks were identified using Ingenuity Pathway Analysis (QIAGEN Redwood City, CA)

knowledgebase and g:Profiler (29). For this, differentially expressed gene identifiers are mapped and analyzed using a one-tailed Fisher Exact Test, (FDR $p < 0.05$). In addition, Gene Set Enrichment Analysis (GSEA Mac App Broad Institute Inc.) (30) was performed using DESeq2-normalized counts with gene set permutation and otherwise default settings. By using the Rat_Gene_Symbol_Remapping_Human_Orthologs-MSigDB v7.2 chip, gene counts were tested against the human hallmark (H), canonical pathways (C2), gene ontology (C5), and immunologic signature (C7) gene sets (version 7.5.2). Gene sets with false discovery rates (FDR) $p < 0.25$ were considered enriched as suggested by GSEA developers. The overlap and connections between the resulting different gene sets were produced by the Enrichment Map Plugin (http://baderlab.org/Software/EnrichmentMap) for Cytoscape 3.8 [19], considering a value of FDR $p < 0.05$. The nodes were joined if the overlap coefficient was ≥ 0.375.

RESULTS

***Hierarchical clustering of 9 independent cDNA libraries*.** For comparative analysis, 9 independent SEP cell cDNA libraries were made from the uninfected and infected cell RNA extracts in experiments using different SEP cell passages for arrest. These libraries were chosen based on the day of the initial increase in Prnp (by RT/qPCR and PrP amyloid western blots), and β-IFN transcripts. Both transcripts rose steeply by 6-8 days after arrest. Arrested cell RNAs and their parallel proliferating controls (**Fig. 1 tif**) were assayed sequentially every 4-6 days for up to 35 days post-arrest [4] at the selected passages and days indicated in Fig 1A. Representative libraries, colored green for uninfected, and red for CJ agent infected, fell into distinct proliferating (lighter shades) and arrested (darker shades) groups (Fig. 1A). The proliferating uninfected normal (Nl) control sets, sampled at 2 different passages (p7 and p25), fell into group 1, and are designated Prol/Nl. These Nl proliferating transcripts were closely related to CJ- proliferating transcripts in group 2 (p17 and p20). Remarkably, despite their prior infection, these CJ- proliferating cells revealed only 19 differentially expressed transcripts (8 up & 11 down regulated). In contrast, comparison of both arrested groups 3 and 4 (Arst/Nl and Arst/CJ+) contained 379 differentially expressed genes. Fig. 1B shows the divergence of the uninfected Nl groups 1 and 3 by principal component analysis along with a clustering of reproducible Prol/Nl vs Arst/Nl differences in independent experimental samples (group 2 proliferating vs group 3 arrested). Notably, the Arst/Nl vs Prol/Nl sets contain more downregulated (blue) than upregulated (yellow) genes in each of the two

p25 Arst/Nl RNAs samples at different days in culture (6 and 14 days). An independent second repeat experiment from p7 also has a highly similar cDNA profile as shown in the Fig. 1B. As in the Arst/Nl controls, Arst/CJ+ cells again segregate in a distinct group from Prol/CJ- cells . However, as shown in Fig. 1C the CJ differential analysis resulted in only 112 differences as compared to 379 in uninfected SEP cells. Moreover, whereas downregulated genes dominated in the Arst/Nl cells, 60% of the transcripts in CJ+ arrested cells were upregulated.

Comparison of proliferating uninfected and CJ- cDNAs. While there were only 19 differences between proliferating Nl and CJ- cell sets, several of them were relevant and suggested stable transcriptional changes caused by prior infection. The Prol/CJ- transcripts reproducibly contained upregulated acute phase protein LPB (up 7.2-fold) involved in innate immunity, and inflammation associated complement C1s (up 3.5-fold in the Prol/CJ- set). Mt1m was also upregulated 5.2-fold, and this zinc binding protein is high in several brain regions and localized to the perinuclear region where PrP amyloid fibrils aggregate in infected cells (6). Six downregulated genes were also notable, including ApoE (down 5.8 fold), Adamts8 metallopeptidase (down 5.8 fold), and Cavin4 (down 9.1 fold) that encodes a Golgi and plasma membrane caveolar protein in synaptic vesicles, and possibly linked to vacuolar “spongiform” dendritic and synaptic changes in TSEs (31). Tspan7, a transmembrane glycoprotein functionally involved in many different viral infections (32) was downregulated 10 fold, and neuron development genes Tenm3 and Dpysl3 were down 19.4 fold and 26.8 fold respectively in Prol/CJ- vs Prol/Nl cells. To best appreciate the diversity and extent of specific changes in the 4 major groups, differential changes between uninfected SEP cells (Arst/Nl and Prol/Nl) are analyzed first, and then the CJ infected samples compared.

Arrest produces abundant transcriptional changes in uninfected SEP cells: To assess reproducibility of changes we compared the 25 most downregulated transcripts in each of the 3 arrested Nl cDNA sets. All these genes were present in at least 2 of these 3 independent samples regardless of function (**Supplement Table S1**). The most downregulated transcripts (5 to 53-fold lower) are suppressed during DNA replication and cell cycle progression, including cell cycle checkpoints, histone synthesis (with 4 different histones lower by 6.5 to 28x) and spindle microtubule formation. A total of 18/25 downregulated genes localized to the nucleus. The longest Nl arrest sample (p25 at 14 days) showed all these genes were downregulated whereas the shorter 6 and

7 day arrested samples displayed some variants (6 and 8 respectively) including two histone transcript clusters that were absent as they normally would be during the S phase of growth. Other minor fold variations in the top 25 transcripts, such as Cenpf, are also consistent with an initial lack of synchrony of G1, S and the shorter mitotic cell cycle phases, and the increased time needed to achieve a complete and stable synchronous arrest in G1. The total differential RNA-seq data further emphasizes multiple processes involved in SEP neuronal arrest were orchestrated precisely and sequentially, as during transitions though DNA replication and mitosis, and all were educed by physiological arrest. Upregulated top genes in Arst/Nl were uniformly changed in all three independent samples (**Table 1 excel**). Three nuclear anti-proliferative upregulated transcripts are seen with diverse other transcripts localized to the plasma membrane or extracellular space, at least in vivo (C1s). Ingenuity pathway analysis showed a very complex network of many replication-related genes and further demonstrated the extent of anti-proliferative upregulated genes in the entire data set. The entire Arst/Nl data can't be graphed with any visual clarity due to all the participating pathways, so an example (from passage 7, day 7 transcripts) is shown in **Fig. 2 tif**.

Neural differentiation genes are upregulated with arrest . 18 highly upregulated transcripts were consistently represented in all three Arst/Nl samples at different times post-arrest (**Table 1 excel**). These upregulated cDNAs were more diversified functionally than those that were downregulated. They included the 1,023-fold upregulated retinol binding protein 2 (Rbp2) active in neuronal differentiation, a calcium channel (Clec2d2) involved in neuronal networks, and Sushi (Svep1) a transcript which encodes a multidomain adhesion protein involved in epidermal differentiation (33) but not yet evaluated in neuronal differentiation. The entire non-selected set of genes highlighted additional neuronal characteristics. **Fig. 3 tif** shows the 4 transcripts with the strongest neuronal effects (darkest red) and 11 other major transcripts activating differentiation of neurons listed (lighter red). Of these, neuregulin 1 (NRG1) and angiotensin receptor 2 (AGTR) promote neurogenesis but have other non-neural actions. However, neuregulin HES6* (Fig. 3), a helix-loop-helix transcription repressor that promotes neuronal differentiation and inhibits astrocyte development (34), is largely limited to brain and endocrine tissue expression. GDF6, another strong contributor to hippocampal neuronal differentiation is also linked to wnt-neural fate (Fig. 4, circle 6). The prion protein gene (PRNP) was also elevated in Arst/Nl cells, in accord with Prnp RNA upregulation previously identified by direct RT/qPCR

analyses. Finally, the Nl neural transcripts appeared to be independent from the upregulated IFNs and inflammatory transcripts. Rather, neuron differentiation here was induced by the anti-proliferative transcripts.

Arrest induces IFN stimulated and innate immunity responses in uninfected cells. Table 1 also shows strongly upregulated immune-associated complement factors Cfh (21 fold) and C1s (8 fold). In these monotypic neural cultures, there is no extrinsic source of complement RNAs so they must be endogenously produced. In addition, the glycoprotein clusterin, a chaperone and complement regulating factor was significantly elevated. Its elevation in Nl arrested cells shows it is not linked to infection. The upregulation of Clu (clusterin) (35) and complement factors was unexpected. However, although not linked to neuron differentiation in the database, complement has been shown to be produced by neuronal cells in culture (36). Analysis of the entire set of upregulated Nl arrest vs proliferating transcripts further expands and highlights distinct transcript sets according to function. Downregulated transcripts were again dominated by anti-proliferative functions as shown in **Fig. S2.** Additionally a small set of RNA processing features, including mRNA splicing, are known to be involved in selecting neuron specific RNA isoforms during neuronal differentiation. Upregulated transcripts fell into a large "anti-viral defense" set that contained innate immune functions (**Fig. 4 tif**, circle 1). Neuronal-linked differentiation transcripts form two separate sets: A) with complement activation and neurite processing/synaptic elaboration (circle 3) and B) Wnt-Neural fate pathways (circle 6). Upregulated anti-proliferative pathways and less specific signaling activities are also seen. Together Figs. 3 and 4 indicate innate immune transcripts separately contribute to neuron differentiation in uninfected SEP cells rather than any anti-viral response.

Ingenuity pathway analyses expanded number of innate immune transcripts linked to neuron differentiation. Many of these highly upregulated anti-viral transcripts are induced by IFNs, especially IFNγ in **Fig. S3** showing strong upregulated viral responsive transcripts including TLR3, TRIM14, RTP4, RSAD2, ISG20, OAS1, GBP4, CD80 and MMP13 as well as multiple weaker IFN-induced transcripts. The extent of this group further verifies the upregulation of β-IFN found previously by direct RT/qPCR (4). It also underscores many additional IFN stimulated transcripts in Arst/Nl cells including IFN-γ, IFN receptor (IFNar), Isg20 and others including upregulated Ifr7 (see complete deposited dataset). Gene Set Enrichment analysis in **Fig. S4** further solidified the strong upregulation of IFNA, IFN-B1 and STAT 1 targets, with corresponding

downregulation of EGFR and G2-M cell cycle signaling. DNA methylation was also downregulated during arrest, consistent with enhanced transcriptional activity of the neural differentiation transcripts identified, rather than a detrimental cell stress or toxic change.

In sum, physiological arrest induced a network of robust IFN responses unrelated to infection that are typically linked to innate immunity. The arrested cells displayed no cytopathic or toxic effects and remained in an arrested state for many days. The interferon network revealed above appears to be integral to the differentiation program at least for some neuronal types, and complement, typically associated with innate immune and anti-viral responses, appears to participate positively in this process. By comparison CJ infected cells, that could not be superficially distinguished from uninfected cells in the proliferative state revealed major global transcript differences affecting proliferative pathways, neural differentiation and several innate immune responses.

Arrested CJ+ versus proliferating CJ- transcripts: As shown in Fig 1C prior CJ infection dramatically changed the latently infected CJ- cell phenotype as evidenced by the reduced scale and range of transcripts can be elicited by arrest. Most differences in this comparison showed up as a failure to inhibit DNA replication and cell cycle checkpoint pathways in arrested CJ+ cells. For example, 23 different histone transcripts were upregulated in both sets of CJ+ cells (at 6 and 34 days with 2 and 10 TCID/cell respectively). This coincided with limited ongoing cell division. In contrast, none of these histones were down regulated in Arst/Nl samples (**Table S1**). The significant downregulation of the ABRA signaling pathway that conveys external signals, including serum signals, further shows escape from the low serum environment that induced complete arrest in uninfected cells. Either CJ- cells were imprinted by previous infection, priming them to escape or resist arrest and/or recrudescence of high infectious agent titers during arrest-activated proliferation pathways. Upregulated proliferative transcripts in CJ+ cells were expected because CJ+ cells had to be split 16-18 days after arrest whereas uninfected cells remained in a non-proliferative state for 27 days (4). The extent and number of proliferative activated transcripts identified here were very large and not anticipated.

Minimized neuronal differentiation in CJ+ cells. Combinatorial comparisons underscored more granular differences including a diminished activation of neuronal transcripts in CJ+ cells. **Fig. 5 tif** compares Arst/CJ+ versus Prol/Nl and Prol/CJ- cells and segregates common and unique cDNAs in uninfected and CJ+

arrested samples. A reduced number of strong neuronal differentiation transcripts is apparent in Arst/CJ+ vs Prol/CJ- sets. This underscores an imprinted or permanent change in latently infected CJ- cells that limits neuron specific development. For example, Wnt (Wnt5a) signaling is upregulated in Arst/Nl cells (Fig. 4) and this transcript positively regulates neuron maturation, synaptogenesis and axonal and dendritic outgrowth. In contrast, the opposite was found in CJ+ samples that showed strong negative regulation of canonical Wnt signaling (**Fig. S5**). Moreover, Cavin4, an important component of synaptic caveolae was upregulated in Nl cells but downregulated in all CJ cells, including proliferating CJ- cells. This is consistent with an imprinted memory that permanently limits synaptic elaboration in latently infected cells.

Combinations of different sets of uninfected and infected samples further expanded major differences in CJ+ and Nl cells as seen in **Fig. 6 tif**. Highest z scores in the Arst/Nl vs Prol/Nl comparison shows strong downregulated (blue) pathways. In contrast, the highest z scores in Arst/CJ+ vs Arst/Nl are upregulated genes that enhance DNA synthesis and cell division, or that have unrelated functional changes. Moreover, five of these same pathways (dotted in red) show opposite regulation between the two sets (Fig. 8, 2 top rows). These examples indicate the depth and range of escape from anti-proliferating signal in CJ+ cells. To complete the comparisons for CJ+ changes, the bottom two sets compare Arst/CJ+ to itself (Prol/CJ-) and to Prol/Nl. These comparisons highlight additional major differences between Nl and CJ+ samples. Notably, the highest CJ+ scores included hyperchemokinemia, caused by viral and other pathogens, cytokine storm signaling transcripts, and proinflammatory Il17 upregulation that promotes and exacerbates viral induced effects. These are not present in the comparable Nl control set with lower upregulated z-scores (Fig. 8, top left). Degradation of extracellular matrix and Matrix Metalloproteinases are also high in this CJ+ set but absent in the Nl set. These CJ+ differences indicate their strong link to high titers of agent rather than to IFN related changes common to both Nl and CJ+ arrested cells.

22 transcripts activate anti-viral activity in CJ+ cells. Ingenuity pathways yielded additional immune and anti-viral distinctions between Arst/CJ+ and Prol/Nl sets. These included both up (red) and down (green) regulated RNAs as indicated by their blue lines. Major strong regulators are listed. The strongest Mx1* gene, induced by IFNs, antagonizes the replication process of several different RNA and DNA viruses. Antiviral HERC6, ISG15, Itgb3 and IFIT 3 were all identified as strong activators in CJ+ cells as shown in **Fig. 7 tif.** This

anti-viral response also revealed a strong interactive network with the IFNs upregulated in the CJ+ dataset and is shown with cellular sites of action (**Fig. S6**). In CJ+ cells the IFNs are not extracellular in origin but made by the cell since no other cells are present to produce activating cDNAs. This data again substantiates RT/qPCR direct experimental results in CJ+ cells: IFNs were far higher than in uninfected cells, indicating IFN enhanced transcripts were activated by the recrudescence of productive infection.

Stronger innate immune and anti-viral patterns in arrested CJ+ vs Nl cells. IPA graphic analysis of signal strength in comparative Nl and CJ+ sets further solidified the above findings as shown in **Fig. 8 tif**. Panel A shows 11 of 16 upstream regulators produced in CJ+ cells (red) are not present in Arst/Nl cells. Panel B shows selected canonical pathways with pathogen induced hyperchemokinemia, cytokine storm, matrix metalloproteinases and Il17 in CJ+ samples. These were not upregulated in Arst/Nl cells.

Unique pathways were further interrogated in both CJ+/Nl and CJ+/CJ- datasets, shown in **Fig. S7**, where plots of additional IPA transcript differences are apparent in both CJ+ comparisons. These transcripts further accentuate viral hypercytokinemia (not present in Arst/Nl vs Prol/Nl comparisons), stronger IFNα/β signaling, rheumatoid arthritis signaling, metalloproteinase activation, degradation of extracellular matrix and O-linked glycosylation that are not present in Arst/Nl samples. Thus during arrest, infected cells recruit an enhanced and more diverse immune response than that found in differentiating normal cells. Interestingly, several of these increases were not seen in CJ+ vs CJ- sample comparisons. This again underscores and expands the underlying changes in CJ- cells imprinted by prior infection that were brought out during re-arrest.

Arrested Nl cells unlike CJ+ cells also displayed robust senescence pathway transcripts in addition to TP53 RNA signaling which regulates transcription of cell death genes. In this case senescence was linked to observed neurodifferentiation rather than cell death or degenerative changes. The widespread down regulation of proliferative elements in Nl cells, but not CJ+ cells, were also evaluated by Gene Enrichment Analysis shown in **Fig. S8**. Analysis of CJ+ vs Arst/Nl also revealed strong upregulation of α and γIFN targets. It also increased methylation, the opposite of the downregulated methylation in Nl cells. Methylation is a major regulator of stable epigenetic changes and methylation of cell cycle checkpoints may be one of the mechanisms that permanently imprint the increased proliferative activity observed in CJ+ cells. CJ+ cells also show strong downregulation of clathrin endocytosis pathways and Cavin4 synaptic vesicle formation, both of which are

reported to be central for PrP processing (37, 38). Neither downregulated genes affected the steep rise in infectivity. The more central and major player in TSE infections, Prnp, was also downregulated 4 fold in Arst/CJ+ cells versus Arst/Nl cells. This RNA-seq data corresponds well with the more specific 5 fold RT/qPCR transcript downregulations previously. Moreover, corresponding PrP and PrP amyloid reductions of 3-5 fold by were also documented in different passages (4) during PrP infection of naïve cells. This is notable because naïve infected cells showed no decrease in PrP. Downregulated Prnp in CJ+ re-arrested samples represent only 1/341 unique CJ+ changes by Venn diagram that shows a complete list of unique CJ+ transcripts **Fig. S9**.

Unique CJ+ vs Arst/Nl show both upregulated (n=195) and downregulated (n=146) transcripts. This more complete data further supports many of the consolidated limited observations depicted above. However, additional transcripts, such as a few upregulated tumor suppressors and neuronal differentiation genes were not picked up by directed queries of IPA analyses, possibly because they have not yet been linked in that database to either neuronal differentiation or inflammation. These additional transcripts could signify a more robust complex network of immune/neuronal differentiation changes. This more detailed supplement also shows the extensive fundamental difference in CJ+ versus other groups along with the limited response of proliferating CJ- versus Nl cells indicates even more profound hidden changes may be induced during prior latent infection. There are only 40 upregulated unique changes induced in arrested CJ- cells (pink column) while there are 86 unique changes in the Nl comparison (light green) as seen in **S10 excel** table. This extensive list can easily be searched for other genes of interest in TSEs, as for example Adamts10 that acts at the cell surface in collaboration with PrP. Downregulated genes show the same pattern, with only 18 differences in CJ- versus 26 in Nl comparisons. In sum, cDNA libraries demonstrated a multitude of previously unrecognized innate immune and anti-viral pathways activated by physiological arrest. Uninfected cells displayed a robust recruitment of neural differentiation transcripts induced during perpetual arrest, along with a surprisingly wide variety of IFN and innate immune pathway responses. These pathways and transcripts were reproducible in independent experiments and appear to be integral to progressive differentiation and not due to underlying cytotoxic or added inflammatory stimuli. Arrest induced changes in latently infected CJ- cells showed marked differences from arrested uninfected control cells in proliferation, neuron differentiation and extent of innate immune responses. Since these CJ+ changes were not induced by arrest of uninfected cells, they are ultimately caused by

infection. Of the many different transcript changes uncovered here, the most dramatic and far-reaching change was the release from proliferation controls in CJ+ cells. These multiple transcripts underlie the partial escape from arrest as compared with the complete arrest of uninfected cells. At the same time CJ+ cells suppressed the neuron differentiation program of normal cells. These CJ+ differences strongly suggested a divergent phenotype imprinted by prior and/or latent infection as discussed below.

In sum, **Fig. 9 tif** shows a graphical abstract of the experimental strategy, comparative data analysis and major reproducible RNA-seq conclusions. As previously shown major biological proliferative changes were expanded were expanded by RNA-seq. Consequences of proliferative arrest were followed by significant neuronal differentiation and immune transcript responses. In comparison with normal uninfected neurons, productively infected CJ+ cells subverted proliferative controls and neuronal differentiation while they enhanced innate immune responses. Moreover, RNA-seq shows that CJ infected cells can remain in a prolonged non-productive latent state, yet they retain imprints of previous productive infection.

DISCUSSION

The ultimate cause(s) of human neurodegenerative diseases, such as Alzheimer's Disease, are difficult to ascertain because critical insults can occur years before symptoms become apparent. Neurons are at the center of pathologic and functional changes while innate immunity can induce latency or accelerate disease progression, especially in hidden viral infections. Because CJD can be latent for 38 years, as in CJD contaminated growth hormone cases, we developed a unique model of latent non-productive infection in neurons that contrasts with shorter latent productive brain infections. Proliferating and arrested neurons were engineered to reversibly differentiate. At 33^0C they proliferate but at 37.5^0C they are arrested. Arrested normal cells produced a plethora of anti-proliferative RNA transcripts. Additionally, known neuron differentiation transcripts, including Prnp were upregulated along with many innate immune responses, including cytokine/chemokine transcripts not previously associated with neuronal differentiation. To generate latently infected CJD cells, high infectivity (CJ+) cells were reverted to a proliferative state at 33^0C and showed no detectable infectivity (CJ-). When these CJ- cells were re-arrested they rapidly developed high infectivity (CJ+), proving they were latently infected. CJ+ neurons downregulated many replication controls, suppressed neuronal differentiation transcripts including Prnp, and enhanced IFN stimulated pathways and anti-viral

transcripts. None of these changes limited productive infection. Latent non-productive CJD infection also epigenetically imprinted many proliferative pathways to thwart complete arrest. In humans, non-productive but infected white blood cells and intestinal or other peripheral myeloid cells may be conditionally stimulated in vitro to reveal latent CJD infection before it spreads to brain. The following discussion focuses on a detailed exposition of the contribution of specific transcripts and pathways that support the global biologic changes observed.

Library cDNA construction with bioinformatics analysis uncovered previously unsuspected actors and global changes that could not be revealed by limited individual RT/qPCR studies. The data here expands the range of centrally involved pathways for proliferative control, neural differentiation, and IFN stimulated and other innate immune transcripts. In normal uninfected cells, conditional physiological arrest induced a total of 379 differentially expressed genes, and the overwhelming majority of the 204 downregulated transcripts suppressed DNA replication. Many upregulated anti-proliferative transcripts further targeted a diverse set of cell cycle checkpoint and mitotic cell transition controls, e.g. by inhibiting G1/S phase and mitotic transitions. These proliferative inhibitory changes were remarkably diverse and virtually complete by 6-7 days and were total by 14 days post arrest in all 3 independent experimental samples collected at 3 different times.

Arrest of normal cells also upregulated known neuronal differentiation transcripts. Ingenuity pathway analysis highlighted 4 strong neuronal transcripts (AGTR2, NRG1, GDF6 and SFRP4) in addition to 11 other neural transcripts including neuregulin, Prnp and HES6. HES6, a helix-loop-helix transcription repressor protein, is mainly transcribed in brain and endocrine tissues and this transcript can participate in epigenetic modifications of proliferation and neurodifferentiation. Arrest also downregulated methylation, another mechanism for epigenetic activation of neuronal transcripts. The basic cell fate of SEP cells was already imprinted when they were engineered to proliferate, and stable neural differentiation transcripts were documented here post arrest. In cultured post-mitotic cerebrum neurons, stable differentiation and stimulus induced changes evaluated over several days revealed selective intron retention in the nucleus linked to neurodiffferentiation (39, 40). Stable nuclear intron change may also be informative for the widespread epigenetic anti-proliferative and innate immune responses brought out by arrest of normal SEP cells here.

Latently infected proliferating SEP cells (CJ-) could not be distinguished from uninfected Nl proliferating cells by their behavior or morphology. Remarkably, these CJ- cells continued to differentially express several relevant transcripts. This indicated that previous and/or latent nonproductive infection was sufficient to change and permanently imprint a CJ altered phenotype. These unique transcripts in CJ- proliferating cells included upregulated acute phase protein LPB, complement (C1s), and Mt1M, an anti-inflammatory molecule (41) along with downregulated Cavin4 and neurodevelopment genes Tenm3 and Dpys13. All of these were indicators of subsequently enhanced inflammatory responses, along with suppressed neurodifferentiation, in re-arrested CJ+ cells.

Re-arrest brought out a variety of imprinted transcriptional proclivities in CJ- latently infected cells. The data here were reproducible in independent culture passages of cells re-arrested at different times up to 34 days. In contrast to Nl cells, high titer arrested CJ+ cells suppressed many Nl proliferative controls and enhanced innate immune cytokine/chemokine and inflammatory transcripts. For many years TSE agents have been considered immunologically silent, largely because they elicit no typical lymphocytic infiltrates that are induced by acute and subacute viral infections. Nor have neutralizing antibodies been found. However, innate immune pathways in CJ+ were significantly enriched compared to Nl arrested cells. Remarkably, the CJ+ ratio of immune to proliferative changes was the reverse of arrested Nl transcripts, with innate immune pathways more upregulated while proliferative pathways were downregulated by infection (see Fig. 6). CJ+ cells also enhanced immune transcripts during the same time that the neuronal differentiation program was suppressed. This indicated that the enhancement of innate immune transcripts in CJ+ was not dependent on neuron differentiation. Previous direct RT/qPCR studies of β–IFN were also validated and expanded in CJ+ cells and included upregulation of many IFNα and IFNγ targets and cytokines. In acute viral infections, such as with Semliki virus, the response of immature neurons is augmented by β–IFN which reduces acute viral replication (42). In contrast, multiple anti-viral transcripts and IFNs here failed to stop rapid CJ agent replication in SEP neurons. We are unaware of any form of recombinant PrP or PrP amyloid that upregulates the IFNs or antiviral transcripts identified here. The enhanced CJ+ anti-viral and IFN activated transcripts observed here may be, at least in part, directly caused by the infectious ~20nm particle (6, 43), or indirectly signaled, as by agent induced dsRNA. Regardless, enhanced innate immune and anti-viral responses coincide with productive infection.

The 4-fold reduction of Prnp transcripts in CJ+ cells also correlated well with previous RT/qPCR and PrP analyses (4), and PrP is an essential protein for productive CJ infection. On the other hand, accumulated PrP amyloid can eliminate CJ infectivity in SEP neurons (5), and the reduction in Prnp and PrP found here may be part of a host defense mechanism imprinted during prior CJ infection. Importantly, naïve SEP cells that were infected previously did not show a reduction in PrP unlike re-arrested SEP cells. Instead, they attained the same 8-10 fold increased PrP as their Nl counterparts (5). This data further supports a retained epigenetic imprint in latently infected CJ- cells. This CJ induced downregulation of Prnp, PrP, and PrP amyloid, in addition to downregulated Cavin4, failed to suppress high levels of infection. Cavin4, caveolar protein in membrane lipid rafts is presumably required for conversion of non-pathogenic PrP to the infectious scrapie amyloid form (38).

Although neurons were originally thought to be the only cells with high infectivity, possibly because they show high levels of PrP amyloid, CJ brain infection activates myeloid microglia and isolation of these living microglia carry infectivity titers equivalent to whole brain homogenates (44) even though they containe barely detectable PrP and no detectable PrP amyloid. Isolated microglia also displayed several IFN regulated and activated genes, e.g., IFI204, IRF2 and IRF8. Several additional immune and inflammatory responses were brought by poly I:C (e.g., ISG15, CXCL10 and OAS) stimulation (45) that correspond to the CJ+ SEP transcripts identified here. Moreover, in CJD infected mouse brains, the IFN linked transcripts IFI204, IFI 202, CXCL10 and IFR8 were elevated as early as 10-40 days post-inoculation, a time of progressive agent doubling. PrP amyloid becomes detectable only 50 days later when infectious titers have risen by 5-6 logs. This very early period of latent infection is rarely studied, and the SEP cell model here shows how critical the conditional changes are for productive infection.

Progressive FU-CJD intracerebral inoculation studies (46) also revealed the cytokines TGFα, IL1β, and MIP-1α and β chemokines were elevated $\geq$10-fold by 30 days. Since none of these changes were present in mice inoculated with uninfected brain, they represent an important recognition by the host of the infectious agent. A similar separation of infectious agent and PrP amyloid effects is seen in progressive rat disease; activated microglia appear midway in the incubation period, and it takes 100 days more for PrP amyloid with spongiform changes to become detectable (8). This further substantiates host innate immune responses to the CJ agent are unrelated to PrP amyloid and neurodegeneration.

While little is known about latency in peripheral cells that are first targeted via natural routes of infection, e.g., via skin abrasion (endemic scrapie) and oral (epidemic BSE) routes, TSE experimental studies clearly show myeloid and lymphoid cells harbor infection for extended times, especially with low dose infections that may not be manifest in brain during an animal's normal lifespan. During this latent period RNA-seq can diagnostically exploit shared immune-linked pathways, especially in accessible infected peripheral immune-related cells such as dendritic gut cells that are infected long before brain (47), and in tonsil and appendix. While infection activated molecules may vary in different cell types and species, their comparable immune-linked functions and overlapping pathways appear to be generalized in a variety of TSE infections (strains and species).

Unlike cell cultures, animals have many additional cellular and humoral ways to hide and restrict TSE agent replication as evidenced by rapid TSE agent replication after infectious transfer from mice to murine cell cultures and visa versa, e.g. (20). A variety of TSE agents consistently double every 19-24 hours in GT1 neuron derived cultures but have dramatically longer clearly different strain-specific 5-25 day doubling times in mice inoculated intracerebrally (23, 48). This underscores release of the infectious agent from complex host controls. When infected cell material is reinoculated in mice these agents again show a vastly slower replication and other strain specific features. Many different host responses, including common lysosomal clearance mechanisms, and PrP amyloid itself, can retard or even eliminate infection in culture (9). But effective inhibitors of TSE agent replication in animals remain uncharted, especially in peripheral lymphoid tissue where these agents silently persist for many years as in kuru and human iatrogenic growth hormone infections.

The multiple modified proliferative transcripts in CJ infected SEP neurons was also remarkable. Re-arrested CJ+ cells subverted proliferative controls, the most profound and global change uncovered by RNA-seq. This led to a partial but permanent escape from arrest in CJ+ SEP cells. Increased cell replication is part of the fundamental biology of TSE infections in both scrapie and CJD and is not limited to neuronal cell types. Although largely forgotten, faster growth of explanted scrapie and CJD infected brain cells are reproducible and reported by at least 4 other independent laboratories (49). Rapidly proliferating permanent cell lines that continue to produce infectivity in addition to those that have lost infectivity were identified. Several of these cell lines showed a transformed immortal phenotype with loss of contact inhibition. Others formed huge tumors

on heterologous transplantation to nude mice. These tumors originated from sCJD human brain cultures and sCJD infected hamster cells (50). This transformation feature, combined with a prolonged non-productive latency, is typical for transforming DNA viruses.

Although there is widespread belief that misfolded PrP amyloid is infectious without any nucleic acid (51), infection by recombinant PrP amyloid ("the gold standard of proof") has not been reproducible, and 20,000 recombinant PrP (recPrP) experiments showed no infection by validated assays, e.g., (52-54), A recent review of an additional 22 recPrP infectivity reports from other laboratories (13) shows the majority failed to produce infection from misfolded recPrP although they did show brain PrP aggregates and PrP "abnormalities" that was not transmissible. While the search for a specifically folded recPrP structure that is infectious continues, many investigators now consider additional component(s) are needed for infection. Nucleic acids would seem likely candidates since they have the capacity to define different stable TSE agent-strains.

While no TSE specific nucleic acid sequence has been delineated, highly infectious ~20 nm infectious TSE particles have been isolated from brain, and these particles do not bind PrP antibodies and correspond to those seen ultrastructurally in cultured cells (6). Gradient isolated infectious particle fractions contain mitochondrial genome contamination in addition to circular DNAs of 1-3kb with phage linked REP sequences (55-57). While only limited nucleic acid sequences have been investigated, an essential nucleic acid component of TSE infectious particles can not be excluded because nucleases that digest nucleic acids destroy 3 logs of infectivity in both CJ and scrapie infectious particles while PrP-amyloid is preserved (14).

The present SEP CJ model is unique because it shows an extended non-productive latency that mimics long non-productive natural and iatrogenic peripheral infections, including CJD human growth hormone infections. We examined only a single human TSE agent-strain; other agents such as sheep derived scrapie, BSE and cervid agents might not show the same pattern of responses even though the fundamental modes of agent spread, latency, and basic brain pathology are common to all TSE strains. Arrest caused far more complex and abundant changes in CJ+ compared to uninfected Nl cells. CJ- cells were primed to respond differently to arrest than Nl SEP cells, i.e., they retained a cellular memory of prior infection. Although the mechanism(s) of imprinting is not clear, methylation patterns were distinct in CJ versus normal SEP neurons. Additionally, others have reported human sCJD and sCJD infected mouse brain transcripts reveal an "epitranscriptomic" profile with

altered RNA edited pathways (58). Such profile changes, along with retained nuclear introns (40), might also provide additional episomal changes in SEP neurons. In any case, accessible latently infected spleen and lymphoid myeloid cells may be conditionally manipulated by stress or arrested by drugs in culture to elicit productive infection. Resulting biological and transcriptional changes such as increased proliferation, or activation of unique transcript patterns that can be rapidly assayed by RT/qPCR, could facilitate diagnosis of latent and/or minimal infection.

The current results bring to the fore many common biologic, virologic and episomally altered activation pathways that may be exploited for targeting latently infected cells. While previous experimental studies have shown productive infection occurs during prolonged non-clinical infections of brain, the above studies demonstrate that infectious TSEs can remain covert in a latent non-productive state. When physiological conditions are altered, these cells can rapidly acquire a highly infectious state. This is relevant for human CJD infections that have a latency of years, a situation that parallels many other established latent infectious agents from tuberculosis to shingles and other viruses. White blood cells and peripheral intestinal and other tissue myeloid cells can disseminate TSE agents to the brain even though they may not be replicating detectable levels of infectious particles (17, 44, 47). The maintenance of non-productive latency is critical for preventing progressive disease.

CONCLUSIONS

Post mitotic neurons are imprinted with a neuronal cell fate. Their neuronal differentiation program here was suppressed when they were reverted from an arrested to a proliferative state. Physiological arrest induced cessation of DNA synthesis and cell proliferation. In normal SEP neurons RNA-seq showed arrest induced a plethora of cell cycle and DNA synthetic transcripts to control proliferation. Sequential time studies further demonstrated simultaneous activation of transcripts for neuronal differentiation, IFNs and other innate immune pathways followed, in accord with previous RT/qPCR assays.

Proliferating neurons with latent CJ infection showed rare transcriptional differences from normal proliferating neurons. However, on re-arrest many normal proliferative cell cycle and DNA synthesis linked transcripts were undermined. Orderly progression of programmed neuronal

differentiation was also subverted whereas innate immune viral-linked transcripts were enhanced. These changes took place before the highest CJ infectious titers (10 infectious particles/cell) were produced at 34 days. Thus prior CJ infection can modulate and/or epigenetically sculp nuclear transcription.

New conclusions here are: 1) normal neuronal differentiation is conditional and encompasses many innate immune responses; 2) Latent non-productive CJ cells escape arrest by subverting numerous histone and cell cycle controls and by strongly upregulating viral pathways including IFNs and cytokine/chemokines; 3) CJ infectious particles accumulate during arrest and induce global cellular changes that are not phenotypically apparent, and not restricted to PrP; 4) an extended latent non-productive state was produced here that is relevant for the many years of covert human TSE infection. This is distinct from the prolonged silent progressive log accumulation of infectious particles post brain inoculations.

REFERENCES

1. Cajal SR. Histologie du Systeme Nerveux de L'homme & des vetebres. Madrid Spain Instituto Ramon y Cajal; 1955.
2. Eves E, Kwon J, Downen M, Tucker M, Wainer B, Rosner M. Conditional immortalization of neuronal cells from postmitotic cultures and adult CNS. Brain Res. 1994;656:396-404.
3. Miyazawa K, Emmerling K, Manuelidis L. Proliferative arrest of neural cells induces prion protein synthesis, nanotube formation, and cell-to-cell contacts. J Cell Biochem. 2010;111(1):239-47.
4. Aguilar G, Pagano N, Manuelidis L. Reduced Expression of Prion Protein With Increased Interferon-beta Fail to Limit Creutzfeldt-Jakob Disease Agent Replication in Differentiating Neuronal Cells. Front Physiol. 2022;13.
5. Miyazawa K, Kipkorir T, Tittman S, Manuelidis L. Continuous production of prions after infectious particles are eliminated: implications for Alzheimer's disease. PLoS One. 2012;7(4):e35471.
6. Manuelidis L, Yu ZX, Barquero N, Mullins B. Cells infected with scrapie and Creutzfeldt-Jakob disease agents produce intracellular 25-nm virus-like particles. Proc Natl Acad Sci U S A. 2007;104(6):1965-70.
7. Büeler H, Aguzzi A, Sailer A, Greiner R-A, Autenried P, Auget M, et al. Mice devoid of PrP are resistant to scrapie. Cell. 1993;73:1339-47.
8. Manuelidis L, Fritch W, Xi YG. Evolution of a strain of CJD that induces BSE-like plaques. Science. 1997;277:94-8.
9. Manuelidis L. Infectious particles, stress, and induced prion amyloids: a unifying perspective. Virulence. 2013;4(5):373-83.
10. Gajdusek DC. Unconventional viruses and the origin and disappearance of kuru. Science. 1977;197:943-60.
11. Croes EA, Roks G, Jansen GH, Nijssen PC, van Duijn CM. Creutzfeldt-Jakob disease 38 years after diagnostic use of human growth hormone. J Neurol Neurosurg Psychiatry. 2002;72(6):792-3.
12. Manuelidis E, Manuelidis L. Clinical and Morphologic Aspects of Transmissible Creutzfeldt-Jakob Disease. In: Zimmerman HM, editor. Progress in Neuropathology. 4. N.Y: Raven Press; 1979. p. 1-26.

13. Ma JY, Zhang JJ, Yan RC. Recombinant Mammalian Prions: The "Correctly" Misfolded Prion Protein Conformers. Viruses-Basel. 2022;14(9).
14. Botsios S, Manuelidis L. CJD and Scrapie Require Agent-Associated Nucleic Acids for Infection. J Cell Biochem. 2016;117(8):1947-58.
15. Wilson DR, Anderson RD, Smith W. Studies in scrapie. J Comp Pathol. 1950;60(4):267-82.
16. Eklund CM, Kennedy RC, Hadlow WJ. Pathogenesis of scrapie virus infection in the mouse. J Infect Dis. 1967;117(1):15-22.
17. Manuelidis EE, Gorgacs EJ, Manuelidis L. Viremia in experimental Creutzfeldt-Jakob disease. Science. 1978;200(4345):1069-71.
18. Fraser HaD, AG. Scrapie in mice. Agent strain diffeences in the distribution and intensity of grey matter vacuolization. J Comp Pathol. 1973;83:29-40.
19. Manuelidis L. Vaccination with an attenuated CJD strain prevents expression of a virulent agent. Proc Natl Acad Sci USA. 1998;95:2520-5.
20. Arjona A, Simarro L, Islinger F, Nishida N, Manuelidis L. Two Creutzfeldt-Jakob disease agents reproduce prion protein-independent identities in cell cultures. Proc Natl Acad Sci USA. 2004;101:8768-73.
21. Manuelidis L, Lu ZY. Virus-like interference in the latency and prevention of Creutzfeldt-Jakob disease. Proc Natl Acad Sci USA. 2003;100: 5360-5.
22. Nishida N, Katamine S, Manuelidis L. Reciprocal interference between specific CJD and scrapie agents in neural cell cultures. Science. 2005;310(5747):493-6.
23. Manuelidis L, Chakrabarty T, Miyazawa K, Nduom NA, Emmerling K. The kuru infectious agent is a unique geographic isolate distinct from Creutzfeldt-Jakob disease and scrapie agents. Proc Natl Acad Sci U S A. 2009;106(32):13529-34.
24. Liu Y, Sun R, Chakrabarty T, Manuelidis L. A rapid accurate culture assay for infectivity in Transmissible Encephalopathies. J Neurovirol. 2008;14(5):352-61.
25. Dobin A, Davis CA, Schlesinger F, Drenkow J, Zaleski C, Jha S, et al. STAR: ultrafast universal RNA-seq aligner. Bioinformatics. 2013;29(1):15-21.
26. Love MI, Huber W, Anders S. Moderated estimation of fold change and dispersion for RNA-seq data with DESeq2. Genome Biol. 2014;15(12):550.
27. Benjamini Y, Hochberg Y. Controlling the false discovery rate: a practical and powerful approach to multiple testing. Journal of the Royal statistical society: series B (Methodological). 1995;57(1):289-300.
28. Subramanian A, Tamayo P, Mootha VK, Mukherjee S, Ebert BL, Gillette MA, et al. Gene set enrichment analysis: a knowledge-based approach for interpreting genome-wide expression profiles. Proc Natl Acad Sci U S A. 2005;102(43):15545-50.
29. Kolberg K, Raudvere U, Kuzmin I, Adler P, Vilo J, Peterson H. g:Profiler—interoperable web service for functional enrichment analysis and gene identifier mapping (2023 update). Nucleic Acids Research.
30. Shannon P, Markiel A, Ozier O, Baliga NS, Wang JT, Ramage D, et al. Cytoscape: a software environment for integrated models of biomolecular interaction networks. Genome Res. 2003;13(11):2498-504.
31. Manuelidis E, Kim J, Angelo J, Manuelidis L. Serial propagation of Creutzfeldt-Jakob disease in guinea pigs. Proc Natl Acad Sci (USA). 1976;73:223-7.
32. New C, Lee ZY, Tan KS, Wong AH, Wang Y, Tran T. Tetraspanins: Host Factors in Viral Infections. Int J Mol Sci. 2021;22(21).
33. Samuelov L, Li Q, Bochner R, Najor NA, Albrecht L, Malchin N, et al. SVEP1 plays a crucial role in epidermal differentiation. Exp Dermatol. 2017;26(5):423-30.
34. Jhas S, Ciura S, Belanger-Jasmin S, Dong Z, Llamosas E, Theriault FM, et al. Hes6 inhibits astrocyte differentiation and promotes neurogenesis through different mechanisms. J Neurosci. 2006;26(43):11061-71.
35. Das Gupta S, Lipponen A, Paldanius KMA, Puhakka N, Pitkanen A. Dynamics of clusterin protein expression in the brain and plasma following experimental traumatic brain injury. Sci Rep. 2019;9(1):20208.
36. Thomas A, Gasque P, Vaudry D, Gonzalez B, Fontaine M. Expression of a complete and functional complement system by human neuronal cells in vitro. Int Immunol. 2000;12(7):1015-23.
37. Shyng SL, Heuser JE, Harris DA. A glycolipid-anchored prion protein is endocytosed via clathrin-coated pits. J Cell Biol. 1994;125(6):1239-50.
38. Vey M, Pilkuhn S, Wille H, Nixon R, DeArmond SJ, Smart EJ, et al. Subcellular colocalization of the cellular and scrapie prion proteins in caveolae-like membranous domains. Proc Natl Acad Sci U S A. 1996;93(25):14945-9.

39. Yeom KH, Pan Z, Lin CH, Lim HY, Xiao W, Xing Y, et al. Tracking pre-mRNA maturation across subcellular compartments identifies developmental gene regulation through intron retention and nuclear anchoring. Genome Res. 2021;31(6):1106-19.
40. Mazille M, Buczak K, Scheiffele P, Mauger O. Stimulus-specific remodeling of the neuronal transcriptome through nuclear intron-retaining transcripts. EMBO J. 2022;41(21):e110192.
41. Dai H, Wang L, Li L, Huang Z, Ye L. Metallothionein 1: A New Spotlight on Inflammatory Diseases. Front Immunol. 2021;12:739918.
42. Narayanan D, Moily N, McQuilten HA, Kedzierska K, Mackenzie JM, Kedzierski L, et al. Immature Brain Cortical Neurons Have Low Transcriptional Competence to Activate Antiviral Defences and Control RNA Virus Infections. J Innate Immun. 2023;15(1):50-66.
43. Manuelidis L. A 25 nm virion is the likely cause of transmissible spongiform encephalopathies. J Cell Biochem. 2007;100(4):897-915.
44. Baker CA, Martin D, Manuelidis L. Microglia from Creutzfeldt-Jakob disease-infected brains are infectious and show specific mRNA activation profiles. J Virol. 2002;76(21):10905-13.
45. Baker CA, Lu ZY, Manuelidis L. Early induction of interferon-responsive mRNAs in Creutzfeldt-Jakob disease. J Neurovirol. 2004;10(1):29-40.
46. Lu ZH, Baker C, Manuelidis L. New molecular markers of early and progressive CJD brain infection. J Cellular Biochem. 2004;93:644-52.
47. Shlomchik MJ, Radebold K, Duclos N, Manuelidis L. Neuroinvasion by a Creutzfeldt-Jakob disease agent in the absence of B cells and follicular dendritic cells. Proc Natl Acad Sci U S A. 2001;98(16):9289-94.
48. Miyazawa K, Emmerling K, Manuelidis L. Replication and spread of CJD, kuru and scrapie agents in vivo and in cell culture. Virulence. 2011;2(3):188-99.
49. Manuelidis E, Fritch W, Kim J, Manuelidis L. Immortality of cell cultures derived from brains of mice and hamsters infected with Creutzfeldt-Jakob disease agent. Proc Natl Acad Sci. 1987;84:871-5.
50. Manuelidis E, Kim, JH, Manuelidis, L. Novel biologic properties of Creutzfeldt-Jacob infected brains in vitro. Katzman R, editor. Cold Spring Harbor, NY: Cold Spring Harbor Laboratory; 1983.
51. Prusiner S. The Nobel Lecture: Prions. Proc Natl Acad Sci U S A. 1998;95(23):13363–83.
52. Timmes AG, Moore RA, Fischer ER, Priola SA. Recombinant prion protein refolded with lipid and RNA has the biochemical hallmarks of a prion but lacks in vivo infectivity. PLoS One. 2013;8(7):e71081.
53. Barron RM, King D, Jeffrey M, McGovern G, Agarwal S, Gill AC, et al. PrP aggregation can be seeded by pre-formed recombinant PrP amyloid fibrils without the replication of infectious prions. Acta Neuropathologica. 2016;132(4):611-24.
54. Schmidt C, Fizet J, Properzi F, Batchelor M, Sandberg MK, Edgeworth JA, et al. A systematic investigation of production of synthetic prions from recombinant prion protein. Open Biol. 2015;5(12):150165.
55. Manuelidis L. Nuclease resistant circular DNAs copurify with infectivity in scrapie and CJD. J Neurovirol. 2011;17(2):131-45.
56. Yeh YH, Gunasekharan V, Manuelidis L. A prokaryotic viral sequence is expressed and conserved in mammalian brain. Proc Natl Acad Sci U S A. 2017;114(27):7118-23.
57. Zur Hausen H, Bund T, de Villiers EM. Infectious Agents in Bovine Red Meat and Milk and Their Potential Role in Cancer and Other Chronic Diseases. Curr Top Microbiol Immunol. 2017.
58. Kanata E, Llorens F, Dafou D, Dimitriadis A, Thune K, Xanthopoulos K, et al. RNA editing alterations define manifestation of prion diseases. Proc Natl Acad Sci U S A. 2019;116(39):19727-35.

Acknowledgments: We are indebted to Brett Robb and NEB for making the ribosomal-deleted RNA-seq libraries. We also thank Najoua Bolakhrif for making the Graphical overview. This work was supported by the Hanna Howard Fund, a gift from the William Prusoff Foundation to LM and in part by NINDS/NIH Award R01NS122907. Access to Partek Flow (Illumina), Qlucore Omics Explorer (Qlucore), and Ingenuity Pathway Analysis (Qiagen) was provided and sponsored by the Cushing/Whitney Medical Library, Yale School of Medicine.

Table & Figures with legends:

			P7, 7d		P25, 6d		P25, 14d		
#	Rat Symbol	Entrez Gene Name	FDR(p)	Log2Ratio	FDR(p)	Log2Ratio	FDR(p)	Log2Ratio	Location
1	Rbp2	retinol binding protein 2	3.67E-02	7.855	9.75E-03	10.813	4.46E-03	11.341	Cytoplasm
2	Sulf2	sulfatase 2	1.61E-04	3.498	2.60E-11	5.515	5.20E-12	5.668	Plasma Membrare
3	Clec2d2	C-type lectin domain family 2, member D	1.42E-05	5.549	2.54E-04	5.329	1.54E-04	5.445	Plasma Membrare
4	Itm2a	integral membrane protein 2A	2.04E-03	3.919	9.20E-06	5.03	1.07E-06	5.344	Plasma Membrare
5	Cfh	complement factor H	3.35E-02	2.701	2.61E-06	5.007	1.15E-07	5.506	Extracellular Space
6	Mmp13	matrix metallopeptidase 13	6.42E-16	6.419	1.70E-07	4.827	4.76E-08	5.017	Extracellular Space
7	Sfrp4	secreted frizzled related protein 4	1.17E-02	3.079	2.48E-04	4.092	6.43E-05	4.329	Plasma Membrare
8	Ephx1	epoxide hydrolase 1	2.04E-03	3.141	2.16E-05	3.969	1.14E-05	4.031	Cytoplasm
9	Ccdc80	coiled-coil domain containing 80	4.02E-02	2.089	1.70E-07	3.899	6.28E-07	3.737	Nucleus
10	Cdkn1a	cyclin dependent kinase inhibitor 1A	4.55E-03	2.597	3.82E-03	3.757	6.71E-03	3.611	Nucleus
11	Svep1	sushi, von Willebrand factor type A, EGF & pentra	9.95E-05	3.588	6.45E-05	3.618	9.41E-07	4.196	Cytoplasm
12	Clu	clusterin	1.12E-06	4.097	7.05E-07	3.585	1.86E-06	4.028	Cytoplasm
13	Abca1	ATP binding cassette subfamily A member 1	4.92E-04	3.37	2.93E-04	3.477	1.54E-04	3.579	Plasma Membrare
14	Mmp2	matrix metallopeptidase 2	1.19E-04	3.108	1.32E-05	3.419	6.40E-06	3.473	Extracellular Space
15	Plk2	polo like kinase 2	3.35E-02	2.759	8.51E-03	3.177	1.18E-02	3.05	Nucleus
16	Tnn	tenascin N	3.83E-04	2.852	1.70E-03	2.964	2.53E-03	2.867	Plasma Membrare
17	C1s	complement C1s	3.76E-04	3.22	4.52E-03	2.891	5.72E-03	2.845	Extracellular Space
18	Edil3	EGF like repeats and discoidin domains 3	3.29E-02	2.492	1.19E-02	2.78	1.88E-03	3.127	Extracellular Space

Table 1: **Consistent upregulation of 18 genes (Log2Ratio) in 3 independent Arst/Nl samples**.

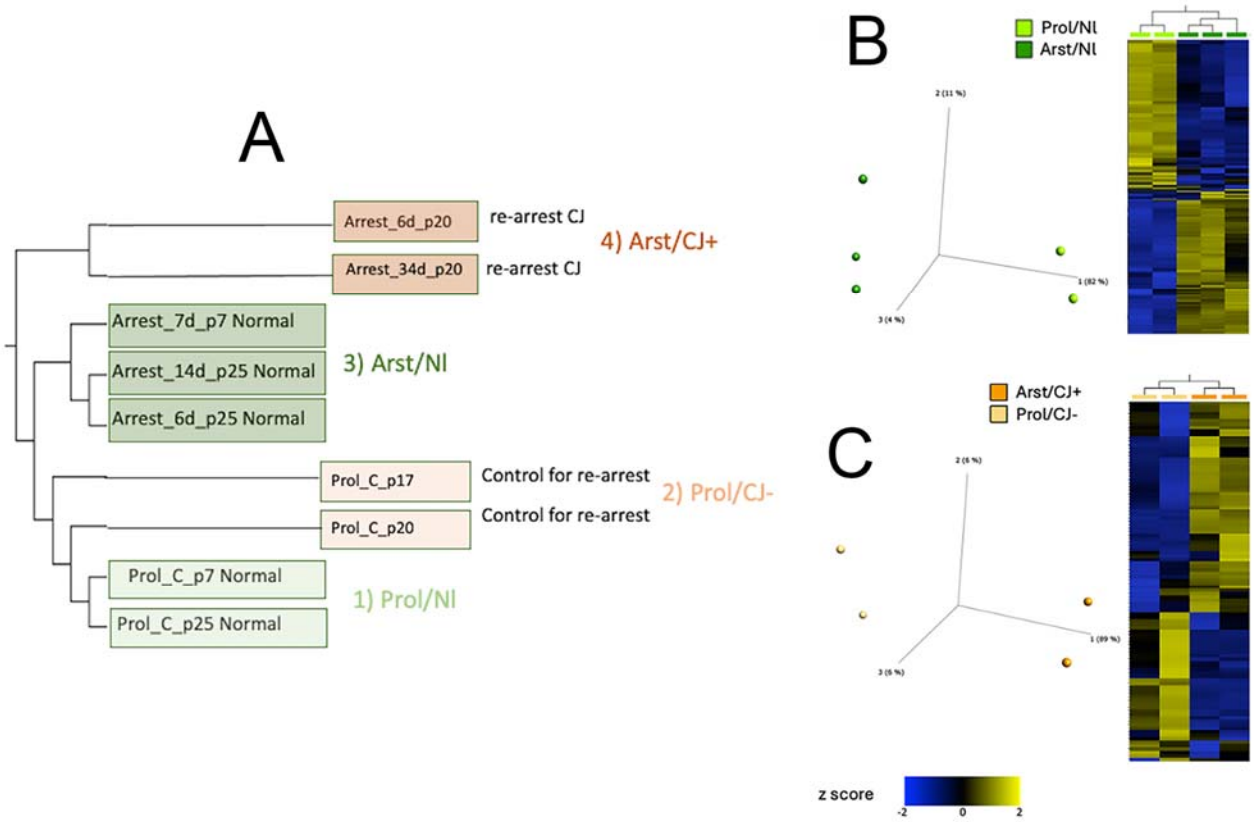

Fig. 1. A): **Hierarchical clustering of different passages (p) and days based on 22,251 normalized genes.** Proliferating Nl controls (Prol/Nl) light green, p7 & p25) were closely related to Proliferating CJ- cells (Prol/CJ-) light red (p17 & p20). Arrested Nl cells (Arst/NL) darker green and arrested CJ (Arst/CJ+) darker red were also more closely related to each other (groups 3 & 4 respectively) than to their proliferating counterparts. **B**): Principal component analysis (PCA) and hierarchical clustering heatmap comparing Nl proliferating and Nl arrested cell sets. DESeq2 differential analysis (FDR $p<0.05$, Fold change>|2|) resulted in 379 differentially expressed genes between these 2 groups (205 downregulated and 174 upregulated). **C**) Principal component analysis (PCA) and hierarchical clustering heatmap comparing CJ- proliferating and CJ+ arrested cell sets yielding a total of 112 differential genes. DESeq2 differential analysis (FDR $p<0.05$, Fold change>|2|) resulted in differentially expressed genes between these 2 groups (45 downregulated and 67 upregulated).

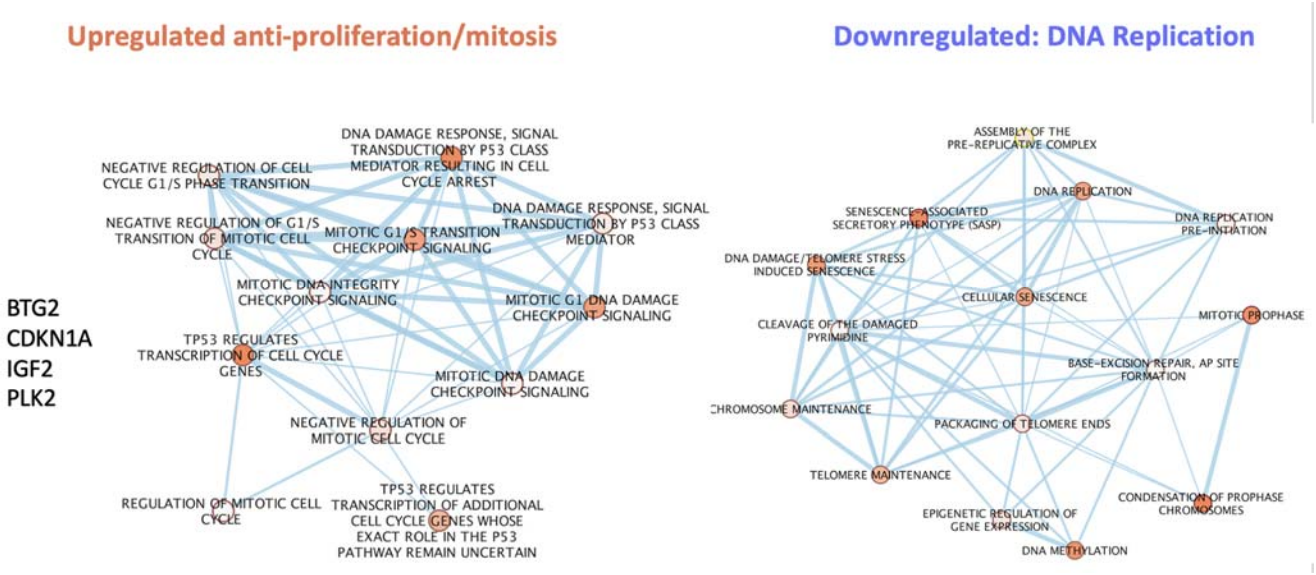

Fig. 2. **Overrepresentation and clustering analysis of enriched pathways contributing to arrest with upregulated and downregulated genes of the p7 day 7 normal sample**. g:Profiler web server was used for overrepresentation analysis. Enriched signatures were analyzed with Enrichment map application and visualized on Cytoscape.

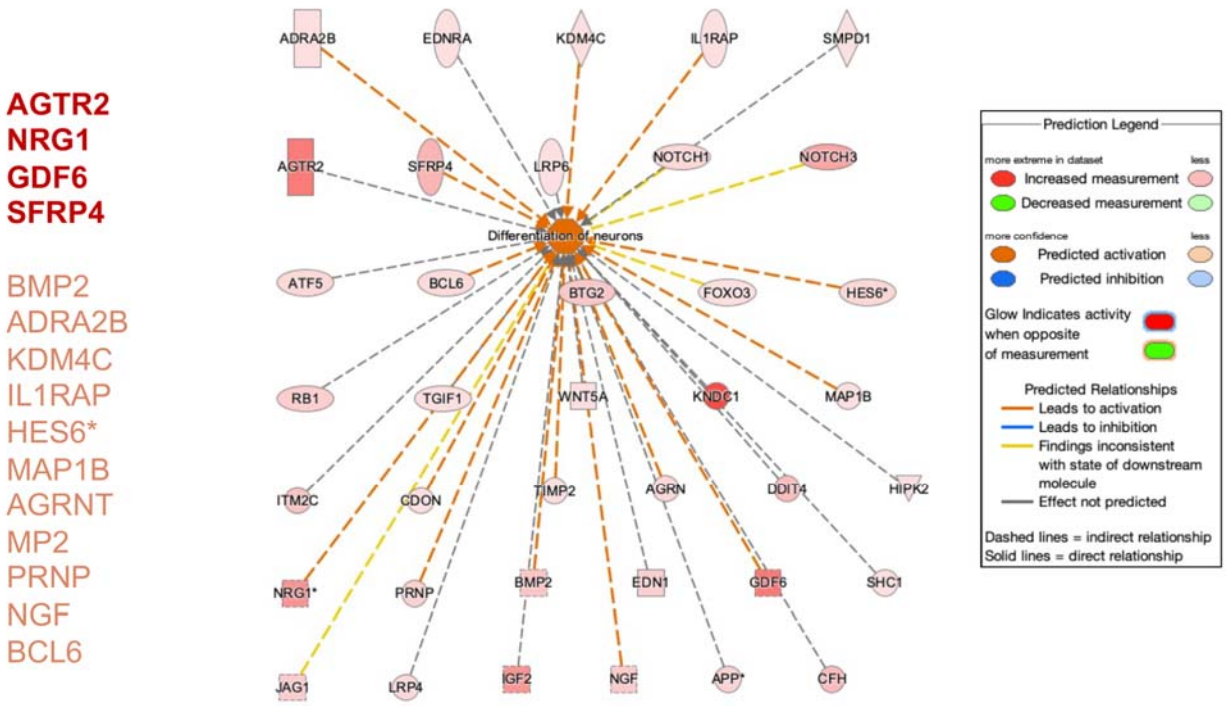

Fig. 3 Ingenuity pathway analysis shows significant overlap (p=1.38E-68) between neuronal differentiation and upregulated differentially expressed transcripts in Arst/Nl samples. Differentiation of neuronal function is predicted to be activated (dark red color). Higher expressed genes are genes shown in darker red color.

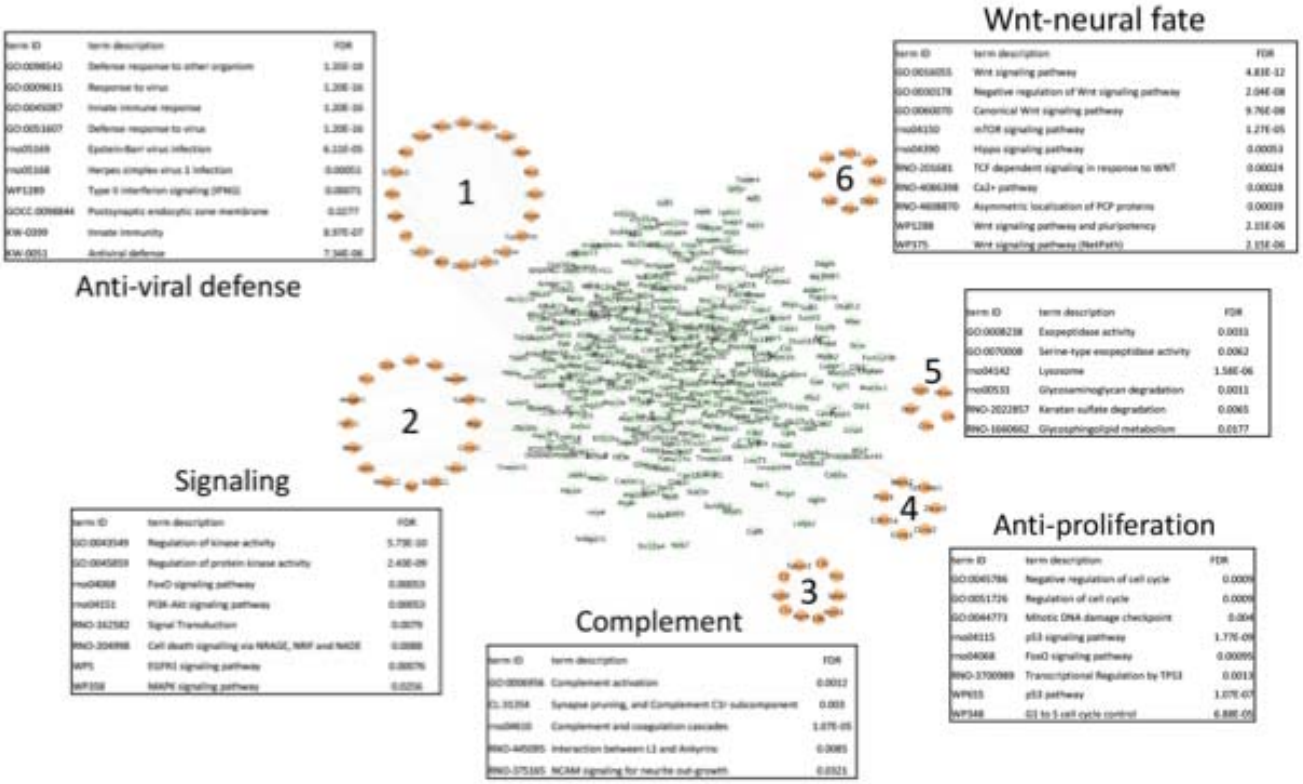

Fig. 4: Interaction network analysis of upregulated differentially expressed genes in Arst/Nl vs Prol/Nl. Interaction network was built using STRING knowledgebase (v. 12.0). The resulting network was imported into Cytoscape (v. 3.10.2), and clustering analysis was performed with MCODE application (v. 2.0.3) using a degree cutoff 2, node density cutoff 0.1, K-core 2, and maximum depth 100. Resulting clusters were functionally annotated on STRING knowledgebase.

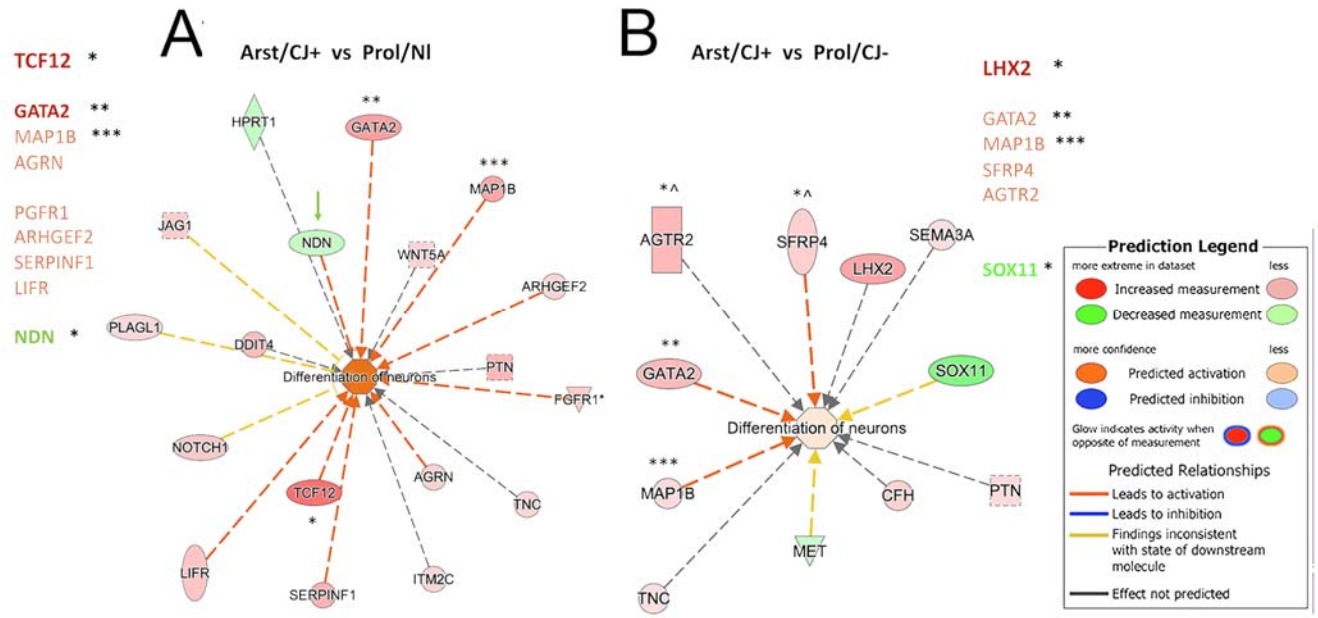

Fig. 5. A) **Ingenuity pathway analysis.** Significant overlap (and activation) between differentially expressed genes and neuron differentiation in Arst/CJ+ vs Prol/Nl cells (A),but it is reduced as compared to stronger activation in Arst /Nl vs Prol/Nl transcripts (see Fig. 3). The differentiation of neurons is even less activating in B) that shows Arst/CJ+ vs Prol/CJ- differences. Note the pale pink center in B with the darker red neuronal activation in A. The transcripts are also different in each of these CJ+ comparisons with only Map18 shared (***) in all 3 comparisons. GATA2 was activated only in these two CJ+ comparisons, but not in Arst/Nl cells (**) , and two stronger transcripts (TCF12 and LHX2) were found only in a single comparison (*). Strong NGR2, GDF6 & SFR4 signals seen in Arst/Nl samples (see Fig. 3) are absent in these CJ+ comparisons and strong Nl AGTR2 is absent or diminished in the CJ+ comparisons above.

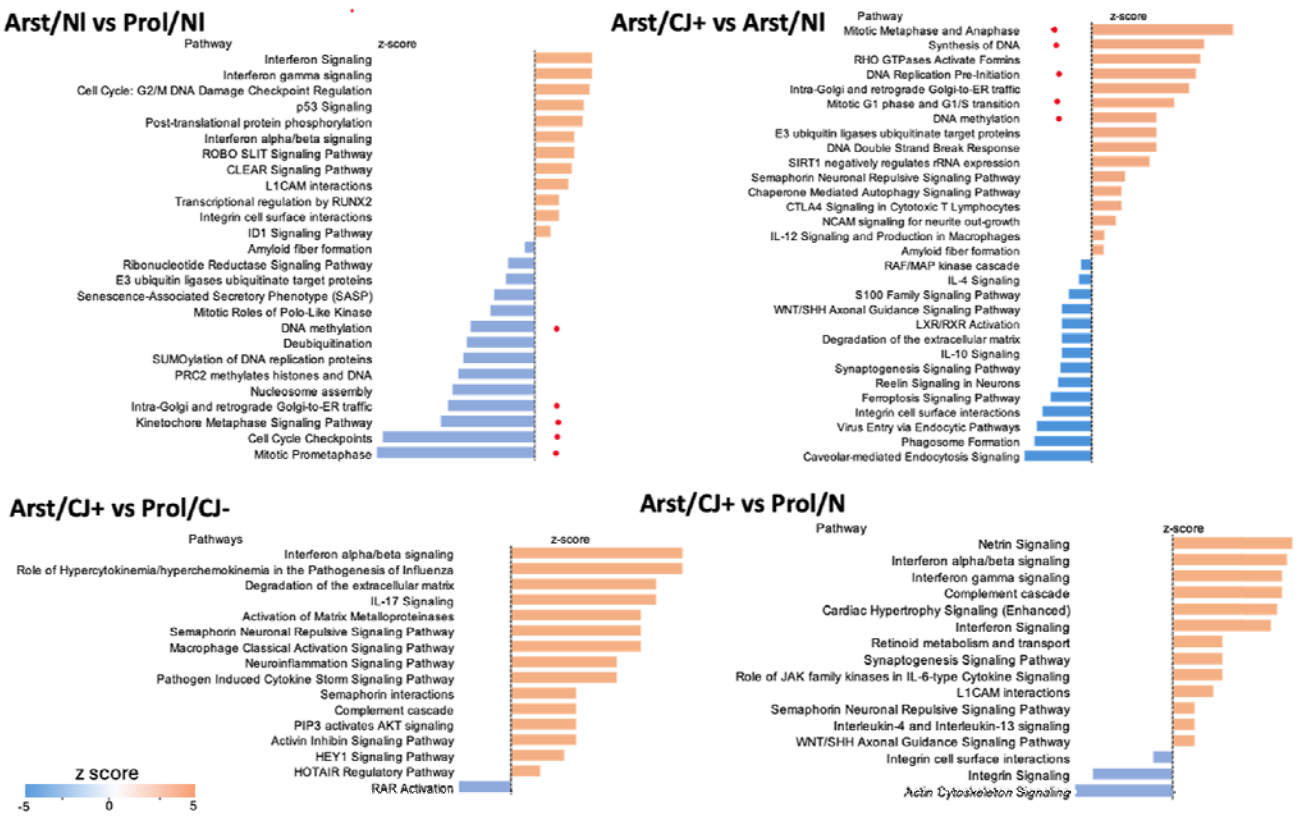

Fig 6. Ingenuity pathway analysis showing overrepresented pathways (Fisher's exact test FDR $p<0.05$), and activation status prediction based on z-score for the comparison of different sets of infected and uninfected cells. Positive z-score (orange bars) indicates pathway activation while negative z-score (blue bars) indicate inhibition.

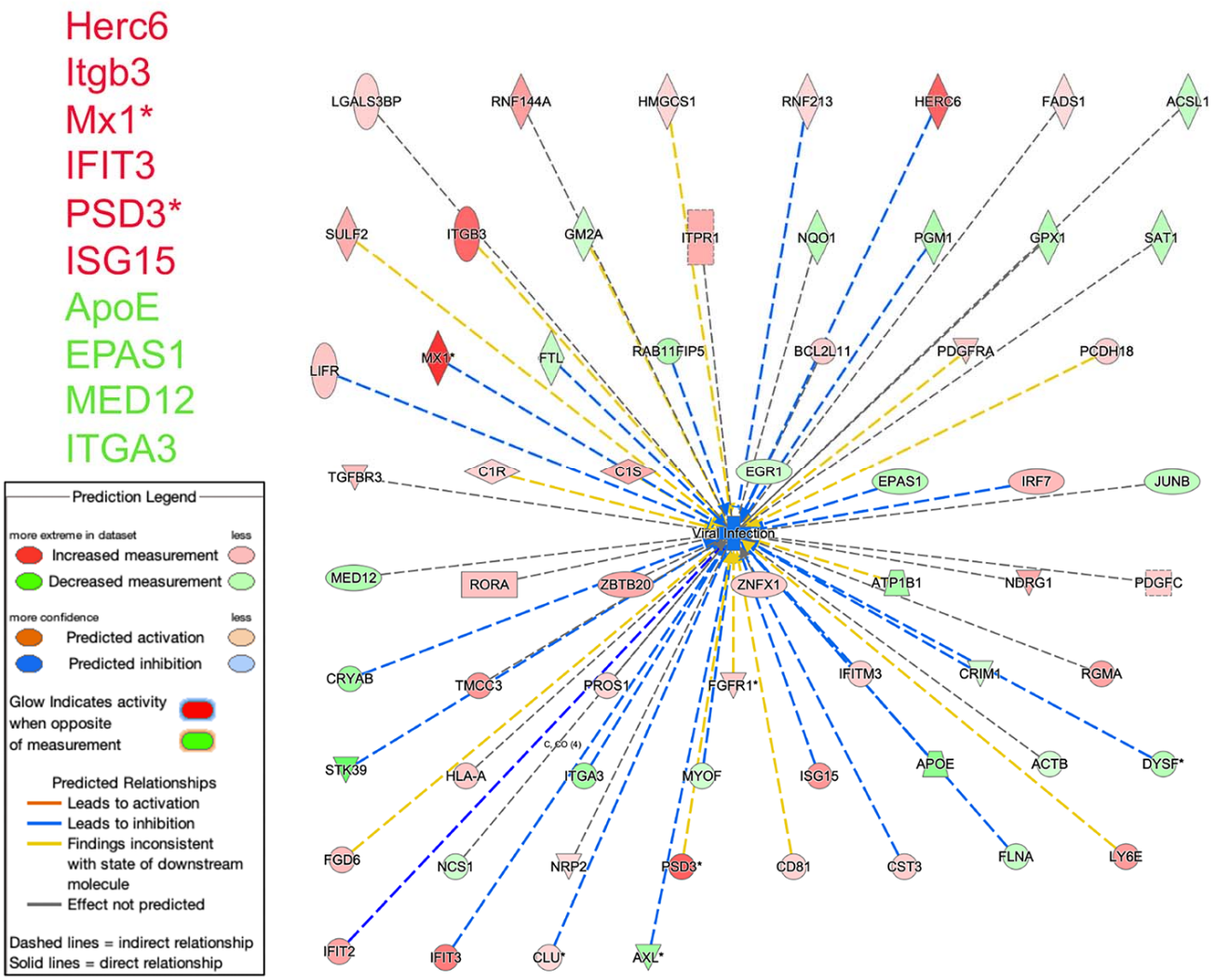

Fig. 7: Ingenuity pathway analysis overlap between differentially expressed genes and viral infection function in Arst/CJ+ vs Prol/Nl. Strong anti-viral activation (blue lines) from transcripts up regulated in CJ+ cells. Mx1 gene protects against viruses that replicate in the nucleus, possibly indicative of a CJ+ DNA component. Although PSD3 (plectin) is captured here by ingenuity viral pathways (without a consistent role), it is highly expressed in neurons but was not IPA linked to neuronal function or differentiation (see Fig. 3).

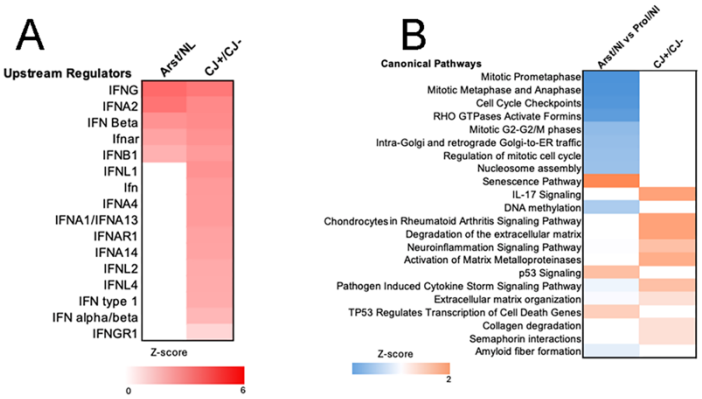

Fig. 8 Ingenuity pathway analysis of upstream regulators. Comparison of upstream regulators and examples of canonical pathways that differ in Arst/Nl and CJ+ cells. A) shows activation status (based on z-score) of expressed upstream IFN regulators (red) not present in Arst/Nl cells. B) shows canonical pathways. Note other signature transcripts upregulated (orange) in CJ such as extracellular matrix regulation. DNA methylation and mitosis are downregulated (blue) in Nl vs CJ.

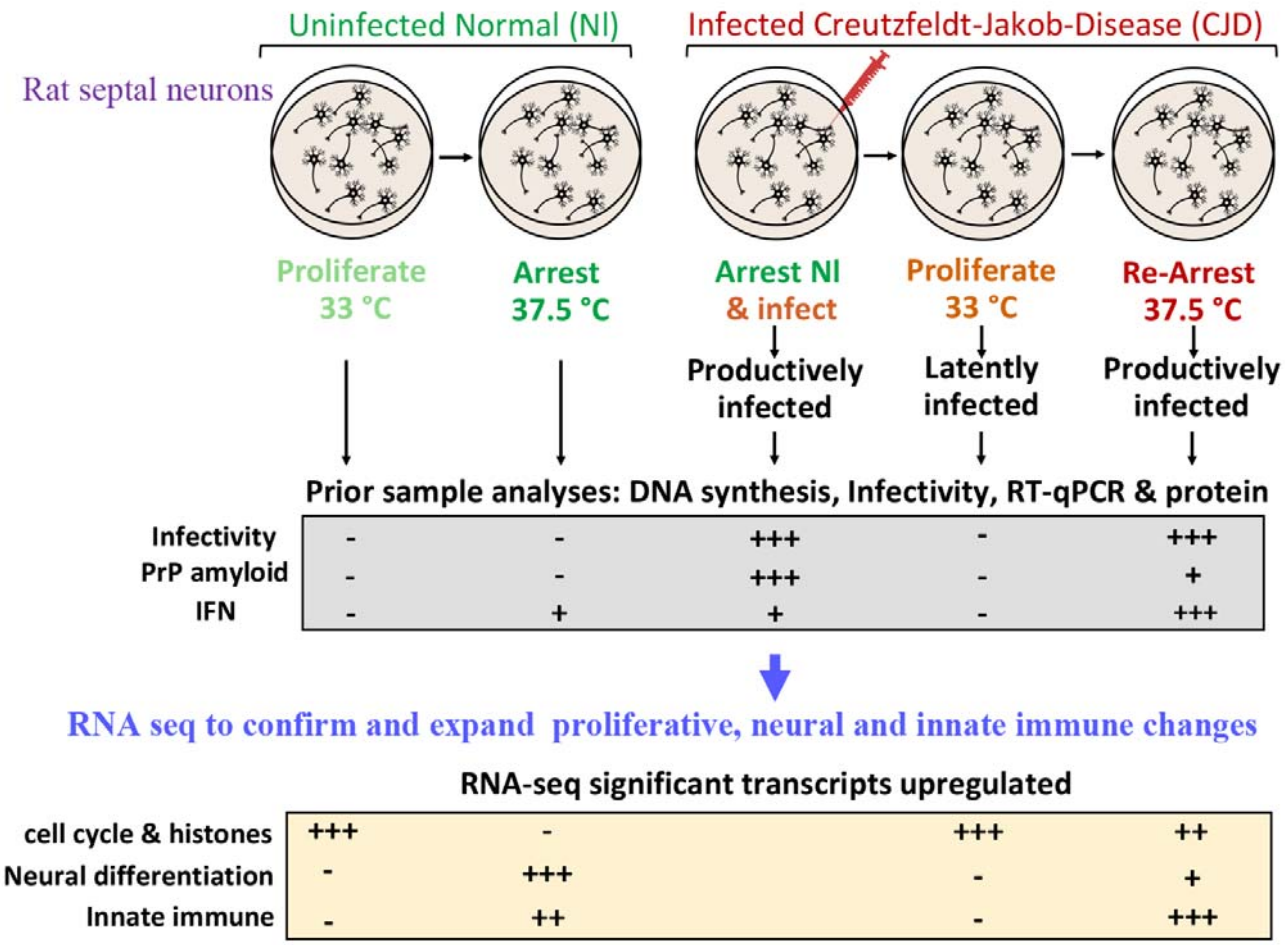

Fig. 9 Graphical summary: Normal rat septal neurons, engineered to reversibly proliferate and arrest DNA synthesis, were compared with CJ infected cells (top row) . Previous DNA experiments, RT/qPCR analyses, prion protein (PrP & PrP amyloid) evaluations, and physiological changes are summarized in the middle row. These finding were confirmed and expanded by RNA seq (bottom row). Numerous major transcriptional differences in normal as compared with latently infected and productively infected neurons were revealed. Abundant cell cycle and histone transcripts controlled normal arrest. This arrest was followed by neuronal differentiation along with upregulated innate immune transcripts. The same conditions of arrest in CJ+ cells subverted cell cycle and histone controls and neural differentiation whereas innate immune responses were enhanced (+++) while – is no change.